A Combined High-, Medium-, and Low-Voltage Test System for Stability Studies with DERs

Francisco Escobar, Jorge García,
Juan M. Víquez, Gustavo Valverde
Engineering Research Institute (INII)
University of Costa Rica
gustavo.valverde@ucr.ac.cr

Petros Aristidou
Department of Electrical Engineering,
Computer Engineering & Informatics
Cyprus University of Technology
petros.aristidou@cut.ac.cy

***Abstract*—Future scenarios with high penetration of Distributed Energy Resources (DERs) call out for detailed network modelling at all voltage levels. The challenges of building a network model that is realistic at both the transmission and distribution levels have led to test systems that use aggregate medium-voltage (MV) loads. In this paper, we present a methodology that uses low-voltage networks with a sensible load allocation to disaggregate MV loads that were previously used in combined Transmission-Distribution (TD) network simulations. The resulting network accurately captures the interaction of transmission and distribution networks, thereby proving useful for new control schemes and stability studies that account for the participation of small and large-scale distributed energy resources. This extended network model is a convenient tool for research, training, and teaching.**

***Index Terms*—Distributed energy resources, modelling, power system dynamics, simulation, synthetic network, test system.**

I. Introduction

In the future, Distribution Networks (DNs) will host a large amount of Distributed Energy Resources (DERs), which are expected to provide ancillary services to Transmission Networks (TNs). This interaction, in turn, requires combined analysis of transmission and distribution systems through co-simulations [1]. However, due to computational burden, it is common practice today to simulate these networks independently, with the DNs aggregated at the substation in TN simulations, and TNs modelled by a Thévenin equivalent in DN studies.

Similarly, when studying scenarios with increased DER penetration, loads and DERs are often aggregated into equivalent models, thus leading sometimes to unrealistic results. Even if the dynamic behaviour is considered in the aggregate models, the individual response of each DER is lost as they do not share the same terminal voltage. This simplification might also lead to unrealistic synchronisation of DER actions and ignores the limitations that individual DERs may face due to physical or local network constraints.

Recently, the IEEE PES Task Force (TF) on Test Systems for Voltage Stability Analysis and Security Assessment published two test systems to be used by researchers [2]. The TF focused on the modelling and dynamics of bulk power systems. According to [3], as DER levels grow, it is not recommended to operate the system with only detailed understanding of large-scale generation and the wider TN network, but also of the response of small-scale generators and flexible loads.

Future DER control schemes that will consider supporting external grids require testing and validation platforms that combine TN and DN models. They will help to assess control schemes and how the individual DER units will receive and process local information to decide when and how to respond. Moreover, as DER are frequently found at Low Voltage (LV) levels, the inclusion of LV network models becomes relevant.

Despite the need for more detailed network models to assess DER integration, utilities use DN models with a limited level of detail. Common causes are the absence of sufficiently granular measurement data, the lack of metering infrastructure [4], and the limited availability of topologies and data of Low-Voltage Networks (LVNs). This situation has led researchers to develop network models from different sources. In [5], a tool was developed for obtaining network models from geographic information systems (GIS). A similar work was done in [6], except that the authors proposed a synthetic network. Their method uses publicly available map data from the OpenStreetMap (OSM) project to create grid models for all voltage levels.

In this paper, we propose a new methodology for building combined HV-MV-LV synthetic systems to be used for testing and validation of future coordination schemes between Transmission System Operator - Distribution System Operator (TSO-DSO). These synthetic systems will facilitate the understanding of complex TN-DN interactions, specially when assessing DER participation in voltage and frequency stability.

Although it is not expected that system operators will have and use such detailed models, due to high computational demands and possible data exchange constraints, these are the only ones that can accurately capture the response of thousands of DERs and flexible loads when the bulk power system is subject to disturbances. The simulation platform will therefore help to better understand the limitations of individual DERs when participating in control schemes and this, in turn, can be very useful to propose more accurate aggregate models

Submitted to the 21st Power Systems Computation Conference (PSCC 2020).

or validate the existing ones. Such control schemes and the comparison between aggregate and detailed DER modelling are beyond the scope of this paper.

This new network is an extension of the system model presented in [7] and is obtained by disaggregating Medium-Voltage (MV) loads into a set of fully-modelled LVNs. Moreover, the network is built in MATPOWER [8] and the source code is available in [9], which makes it a convenient tool for research, training, and teaching. The simulations presented in this paper were carried out in RAMSES, an academic, time-domain, dynamic simulation software [10].

This paper is organised as follows. Section II describes the base templates used for building the network. Section III presents the four-step methodology used for choosing the subset of those templates that is best suited for disaggregating a given MV load. Section IV then presents and discusses the results of applying that methodology to a combined Transmission-Distribution (TD) system and Section V provides key conclusions.

II. Description of base templates

In this section, we present the High-Voltage (HV), MV, and LV templates that are used as a starting point for synthesising a network with all three voltage levels combined.

On the one hand, the HV template is a variant of the Nordic32 test system, which is documented in [2] and whose one-line diagram is shown in Fig. 1. This system was chosen as it is limited by voltage instability and includes all components that play a significant role in this phenomenon [2]. In the original model, the MV distribution networks are modelled by aggregate loads. There are 32 transmission buses, 22 distribution buses, and 20 generator terminal buses, for a total of 74 buses. Also, there are 102 branches, which include 22 step-down and 20 step-up transformers. On the other hand, the MV template is a 11 kV radial network developed by the Centre for Sustainable Electricity and Distributed Generation in the UK [11]. Its one-line diagram is shown in Fig. 2. The network contains 75 buses and 74 branches, one of which is a step-down transformer.

Contrary to the case of the HV and MV networks, which are built each from a single template, the LVNs are chosen from a larger template set. This work uses 14 three-phase 0.4 kV radial networks, developed and documented in [12]. The number of buses per template ranges from 97 to 321, while the number of load buses ranges from 48 to 165. The topologies were extracted from a GIS database and the line parameters of the corresponding Π models were obtained from the line geometries. As the target synthetic network is intended for stability studies, the LVNs are supposed to be balanced and hence only positive-sequence impedances are considered. In order to speed up subsequent simulations, the topologies were modified by removing null power injection buses, which also results in less branches. The simulation-time reduction derived from this step is substantial, as the proposed disaggregation methodology relies on the repeated calculation of power flows.

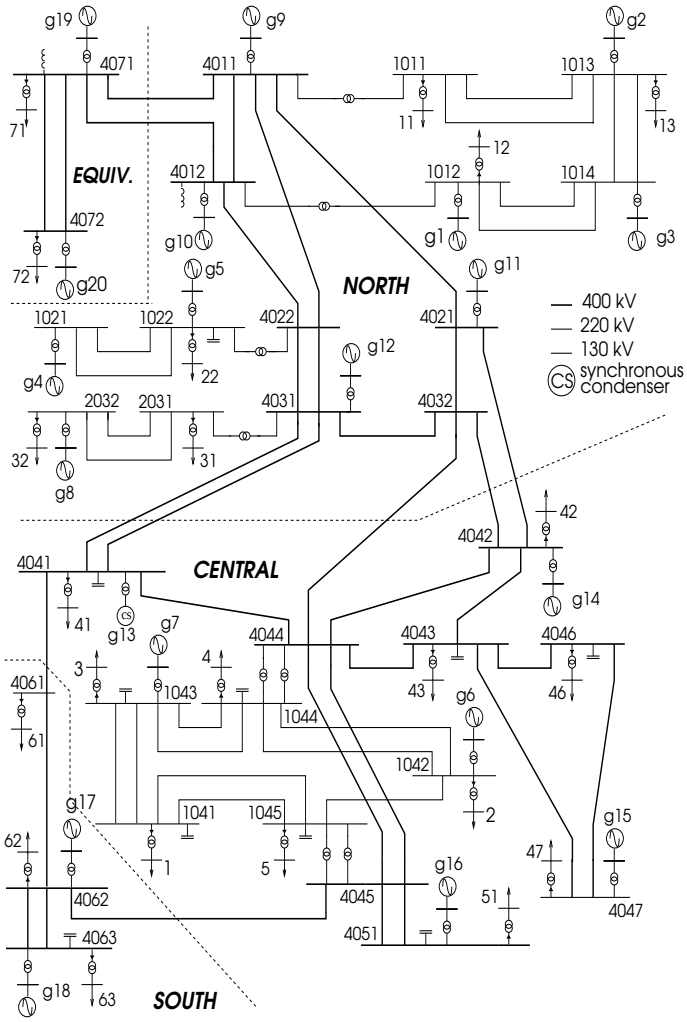

Fig. 1. One-line diagram of the base template for the HV network [2].

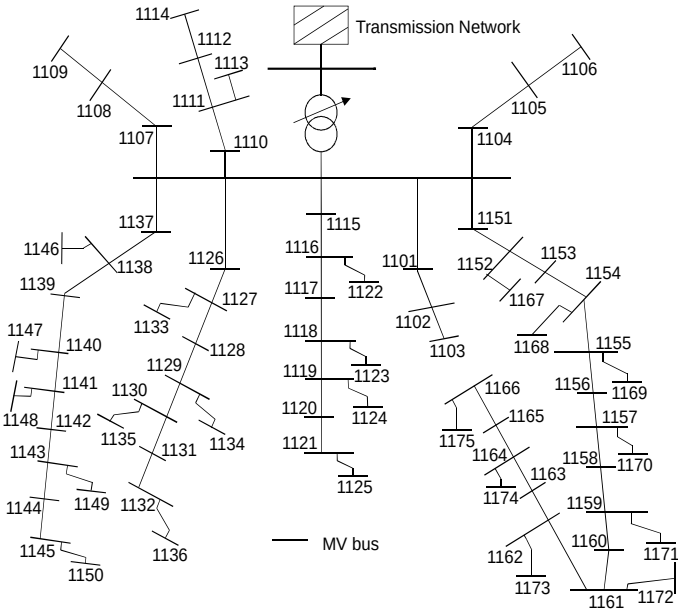

Fig. 2. One-line diagram of the base template for the MV networks [11].

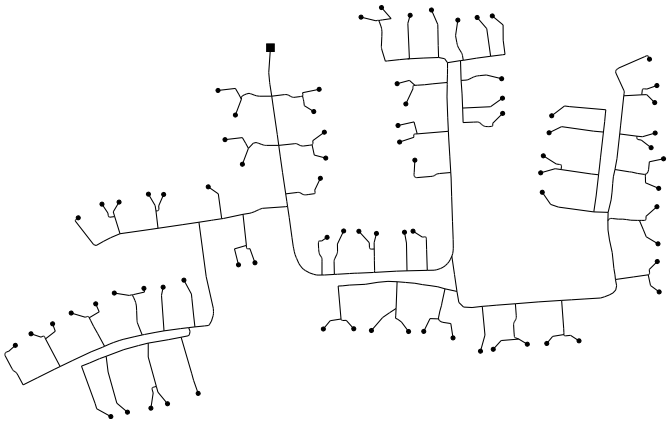

Fig. 3. One of the 14 LVNs that were used in this work as base templates. It is fed by a MV/LV transformer (■) and it contains 79 load buses (•).

In the present work, each LVN template is fed by a $500\,\mathrm{kVA}$ MV/LV transformer with nominal voltages of $11\,\mathrm{kV}/0.4\,\mathrm{kV}$ and five tap positions in the range of $\pm 5\%$. The series resistances of all transformers are uniformly distributed between 1% and 2% in the transformer's base, while the series reactances are uniformly distributed between 6% and 8%. Figure 3 shows one of the resulting LVNs.

III. Methodology

In this section, we present a four-step methodology for disaggregating MV loads into LVNs. First, the base LVN templates from the preceding section are modified in order to obtain a larger and more diverse template set. Second, different DERs and loads are allocated throughout each template. Third, given the demand at the feeder of each template due to the DER and load allocation, the subset of templates that consumes the closest power to the aggregate load is chosen. Fourth and last, each template undergoes a fine-grained load reallocation that causes its total demand to match exactly the aggregate load while keeping a similar DER and load allocation. This methodology is applied to each of the MV loads in the TD network. This work takes as a starting point the system presented in [7], referred to in the following as the bulk power system. A more detailed description of these steps is presented in the following.

A. Diversification of base templates

If the number of available LVN templates is small, it could be necessary to make substantial changes to the original load allocation in order to disaggregate the MV loads. Furthermore, different MV loads could be disaggregated into the same LVNs, which would lead to a system with an unrealistic topology. Since the number of base templates can be limited by external factors, such as the public availability of topologies and line parameters, this work proposes the modification of the existing templates as a way to diversify the template set.

The criterion used to modify a template T_k is the number of load buses that the new templates should contain. In order for the resulting template set to be more diverse, these numbers should be uniformly distributed between a maximum and a minimum. We denote the set of load buses of template T_k as $\mathcal{L}_k$ and its cardinality as $|\mathcal{L}_k|$. Then if, the resulting diverse template set $\mathcal{T} = \{T_1, T_2, \ldots, T_n\}$ is such that $|\mathcal{L}_i| \leq |\mathcal{L}_k|$ whenever $i \leq k$, then all $|\mathcal{L}_k|$ should be uniformly distributed between $|\mathcal{L}_1|$ and $|\mathcal{L}_n|$. This is achieved by setting the desired number N of additional templates as a parameter and by generating a random sequence $a_1, a_2, \ldots, a_N$ of integers that are uniformly distributed between $|\mathcal{L}_1|$ and $|\mathcal{L}_n|$. Then, for $1 \leq i \leq N$, a template with exactly a_i buses is obtained from one of the base templates. This is done by randomly removing a total of $|\mathcal{L}_k| - a_i$ load buses from the base template T_k whose set $\mathcal{L}_k$ of load buses satisfies $|\mathcal{L}_{k-1}| \leq a_i < |\mathcal{L}_k|$. Then, this new template is included as part of the available set. Each time a load bus L is removed from T_k, the lines connected to this load bus L are also removed.

B. DER and load allocation

Once a large template set $\mathcal{T}$ is available, DERs and loads are allocated at each load bus L in $\mathcal{L}_k$ of each template T_k in $\mathcal{T}$ in such a way that the power consumed at L is realistic. This step is critical as the micro-level allocation of DERs and loads is what determines the system response to disturbances and control actions. Given a set $\mathcal{D}$ of available DER and load types, three consecutive decisions are taken: whether a DER or load of type d in $\mathcal{D}$ is connected to L, whether the DER or load is on or off, and finally, when turned on, how much power does the DER (resp. load) generate (resp. demand).

Taking the first decision means defining a logic function $\Omega\colon \mathcal{L} \times \mathcal{D} \to \{\textsc{True}, \textsc{False}\}$ such that

$$\Omega(L, d) = \begin{cases} \textsc{True} & \text{if a DER or load of type } d \text{ is connected to } L, \\ \textsc{False} & \text{otherwise.} \end{cases}$$

This function is implemented by defining a fraction f_d of load buses that will contain DERs or loads of type d and then randomly allocating those DERs or loads throughout the LVN.

Taking the second decision means instead defining a function $\Gamma\colon \mathcal{L} \times \mathcal{D} \to \{1, 0\}$ such that

$$\Gamma(L, d) = \begin{cases} 1 & \text{if DER or load of type } d \text{ at } L \text{ is on,} \\ 0 & \text{otherwise.} \end{cases}$$

In order for the allocation to be representative of the steady state, Γ should be chosen to be 1 with a probability π_1 equal to the duty cycle of the DER or load of type d at L and 0 with a probability $1 - \pi_1$. This is particularly important for thermostatically-controlled loads (TCLs), which constantly switch on and off. For instance, the duty cycle of conventional air conditioning (AC) units is close to 20%, as reported in [13]. Therefore, the probability that a given AC unit is on at some particular time should be assumed to be $\pi_1 = 0.2$.

Finally, taking the third decision means defining a function $p_{\mathrm{nom}}\colon \mathcal{L} \times \mathcal{D} \to \mathcal{P}_d$, where $\mathcal{P}_d$ is a set of predefined nominal active powers for a given DER or load type d in $\mathcal{D}$, and a similar

function $q_{\text{nom}}\colon \mathcal{L} \times \mathcal{D} \to \mathcal{Q}_d$, where $\mathcal{Q}_d$ is a set of predefined nominal reactive powers. In general, it is not true that each DER will demand a predefined nominal power $p_{\text{nom}} + jq_{\text{nom}}$ at any given voltage, but this approximation simplifies the load disaggregation by decoupling the power flow calculation from the DER and load modelling.

Given the three preceding functions, the DER or load of type d at the load bus L demands an active power

$$p(L,d) = \begin{cases} \Gamma(L,d)p_{\text{nom}}(L,d) & \text{if } \Omega(L,d) = \textsc{True}\,, \\ 0 & \text{if } \Omega(L,d) = \textsc{False}\,, \end{cases}$$

and a reactive power

$$q(L,d) = \begin{cases} \Gamma(L,d)q_{\text{nom}}(L,d) & \text{if } \Omega(L,d) = \textsc{True}\,, \\ 0 & \text{if } \Omega(L,d) = \textsc{False}\,. \end{cases}$$

The total demand of the template T_k can therefore be found by defining each load bus L_i as a PQ bus with a demand

$$x_{pi} = \sum_{d \in \mathcal{D}} p(L_i, d) \quad \text{and} \quad x_{qi} = \sum_{d \in \mathcal{D}} q(L_i, d).$$

The primary-side bus of the MV/LV transformer is set as the slack bus with a voltage of $1\,\text{pu}$ and the transformer is assumed to operate at its nominal tap position r_0. Then, the total complex power $P_k + jQ_k$ consumed by the LVN is found through a power flow study. Most MV buses, however, operate at voltages different than $1\,\text{pu}$, which means that the demand of the LVN templates will change. Nevertheless, $P_k + jQ_k$ serves as a first estimate in order to know which templates to choose in the first place.

C. Template selection

At this point, a choice is made regarding which templates from $\mathcal{T}$ are used to disaggregate a given MV load $S = P + jQ$. This is solved by finding a set $\mathcal{M} \subseteq \mathcal{T}$ such that

$$\Sigma = \sum_{T_k \in \mathcal{M}} P_k + jQ_k$$

is as close as possible to S according to some metric $\mu_1(S, \Sigma)$. Note that Σ is the demand of $\mathcal{M}$ when all of its templates are fed by a slack bus voltage of $1\,\text{pu}$.

From this perspective, if all powers are expressed in such units that they can be represented with enough accuracy by integers, then the search for the optimal subset $\mathcal{M}^\star$ is an instance of the multi-dimensional subset sum problem.

Although an exhaustive search would run in time $O\left(2^n\right)$ for $n = |\mathcal{T}|$, this problem lends itself to an approach based on Dynamic Programming (DP) [14] that runs in time $O\left(|P||Q|n\right)$. Let $\mathcal{M}^\star(i,p,q)$ be the subset of $\mathcal{T}$ that contains, at most, the first i templates in $\mathcal{T}$ and whose demand $\Sigma^\star(i,p,q)$ when fed by a slack bus voltage of $1\,\text{pu}$ is as close as possible to $p + jq$ according to μ_1 without exceeding neither p nor q. The original problem is then equivalent to finding $\mathcal{M}^\star(n,P,Q)$. This can be accomplished by starting from the base cases $\Sigma^\star(0,p,q) = \Sigma^\star(i,0,0) = 0$ and solving the recurrence relation

$$\Sigma^\star(i,p,q) = \begin{cases} \Sigma_1 & \text{if } p < P_i \text{ or } q < Q_i, \\ \textsc{opt}(\Sigma_1, \Sigma_2) & \text{otherwise,} \end{cases} \tag{1}$$

where $P_i + jQ_i$ is the individual demand of template T_i, the total demands $\Sigma_1 = \Sigma^\star(i-1,p,q)$ and $\Sigma_2 = P_i + jQ_i + \Sigma^\star\left(i-1, p-P_i, q-Q_i\right)$ are, at each step, the two candidates to be closest to $p + jq$, and where the function $\textsc{opt}(\Sigma_1, \Sigma_2)$ is equal to Σ_1 if $\mu_1(S,\Sigma_1) \leq \mu_1(S,\Sigma_2)$ and to Σ_2 otherwise. The recurrence relation (1) makes it possible to obtain not only $\Sigma^\star$, but also $\mathcal{M}^\star$, since $\textsc{opt}(\Sigma_1, \Sigma_2)$ returns Σ_1 when $T_i \in \mathcal{M}^\star$ and Σ_2 when $T_i \notin \mathcal{M}^\star$. Thus, the solution $\mathcal{M}^\star$ can be built by keeping track of the output of the function $\textsc{opt}$. Moreover, if there is an alternative template set $\mathcal{T}'$ whose n' templates demand negative power, this approach can be used to disaggregate negative MV loads by searching for $\mathcal{M}^\star(n', -P, -Q)$.

The metric $\mu_1(S,\Sigma)$ should be any meaningful measure of the mismatch between S and Σ. This work uses $\mu_1(S,\Sigma) = \|S - \Sigma\|$, which is the Euclidean distance between S and Σ in the complex plane. However, different weights could be assigned to the mismatches of the real and imaginary parts so as to penalise more the differences in active or reactive power.

Since the DP approach always finds the optimal solution and is, therefore, deterministic, several MV loads could be disaggregated into the same LVNs if the loads were similar to each other and if the same set $\mathcal{T}$ was used during each disaggregation. This is solved by using a random subset of $\mathcal{T}$ for each MV load. The time required to find such a subset is small in comparison to the optimisation process. Furthermore, the detriment to the optimality, namely the increase in $\mu_1(S,\Sigma^\star)$, is negligible when the initial set $\mathcal{T}$ is large enough. Another shortcoming of the DP approach is that it finds the optimal subset $\mathcal{M}^\star$ without any restriction on its cardinality $|\mathcal{M}^\star|$. This is solved by setting a maximum number $\bar{n}$ of templates that can be used to disaggregate a MV load, and by removing recursively from $\mathcal{T}$ the template with the lowest active (resp. reactive) power demand in $\mathcal{T}$ if there are $\bar{n}+1$ templates in $\mathcal{T}$ whose total demand does not exceed P (resp. Q). Lastly, all templates whose demand exceeds either P or Q are removed as they cannot possibly belong to $\mathcal{M}^\star$. This removal reduces the running time of the DP solution.

D. Connection to bulk power system

Once $\mathcal{M}^\star$ has been found, each of its templates undergoes a fine-grained load reallocation that causes them to consume collectively the exact aggregate load $S = P + jQ$. This reallocation is needed because $\mathcal{M}^\star$ was chosen on the basis of the demand of its templates when fed by a voltage of $1\,\text{pu}$ and also because $\Sigma^\star$ was not necessarily equal to S.

The demands x_{pi} and x_{qi} at each load bus L_i in $\mathcal{L}_k$ are modified in each template T_k in order for $\Sigma^\star$ to be equal to S when they are connected to the MV bus at an arbitrary voltage $V\angle\varphi$. This is achieved by ensuring that each T_k, which previously consumed $P_k + jQ_k$, now consumes $P_k P/\operatorname{Re}(\Sigma^\star) + jQ_k Q/\operatorname{Im}(\Sigma^\star)$ when each L_i is a PQ bus with load $x_{pi} + jx_{qi}$. This guarantees an exact disaggregation as the total demand would then be

$$\sum_{T_k \in \mathcal{M}^\star} P_k P/\operatorname{Re}(\Sigma^\star) + jQ_k Q/\operatorname{Im}(\Sigma^\star) = S. \tag{2}$$

If $\mathbf{x}'_p = (x'_{p1}, \ldots, x'_{p|\mathcal{L}_k|})$ and $\mathbf{x}'_q = (x'_{q1}, \ldots, x'_{q|\mathcal{L}_k|})$, then the condition (2) can be expressed as two separate equality constraints $g_P(\mathbf{x}'_p, \mathbf{x}'_q) = 0$ and $g_Q(\mathbf{x}'_p, \mathbf{x}'_q) = 0$.

For the resulting templates to be realistic, the new demands $\mathbf{x}'_p$ and $\mathbf{x}'_q$ are chosen so as to minimise a global metric μ_2 that measures how much they differ from the original allocation. This work uses

$$\mu_2(\mathbf{x}'_p + j\mathbf{x}'_q, \mathbf{x}_p + j\mathbf{x}_q) = \left\|\mathbf{x}'_p - \mathbf{x}_p\right\|^2 + \left\|\mathbf{x}'_q - \mathbf{x}_q\right\|^2.$$

Furthermore, since the target synthetic network is intended for stability studies, bus voltages close to $1\,\mathrm{pu}$ are desired at the beginning of the simulations for all voltage levels. The voltage magnitude v_i at each bus must therefore satisfy $\underline{v} \leq v_i < \bar{v}$ for some bounds $\underline{v}$ and $\bar{v}$. Finally, in order for the new demands x'_{pi} and x'_{qi} to accommodate the DERs and loads that were originally connected to the load bus L_i, the new demands must satisfy $x_{pi} < x'_{pi}$ and $x_{qi} < x'_{qi}$. The preceding constraints for voltage and demand can be expressed as $h(\mathbf{x}'_p, \mathbf{x}'_q) \leq 0$.

In these terms, the load reallocation in any template T_k can be formulated as an Optimal Power Flow (OPF) problem of the form

$$\begin{aligned} \min_{\mathbf{x}'_p, \mathbf{x}'_q} \quad & \mu_2(\mathbf{x}'_p + j\mathbf{x}'_q, \mathbf{x}_p + j\mathbf{x}_q) \\ \text{subject to} \quad & g_P(\mathbf{x}'_p, \mathbf{x}'_q) = 0, \\ & g_Q(\mathbf{x}'_p, \mathbf{x}'_q) = 0, \\ & h(\mathbf{x}'_p, \mathbf{x}'_q) \leq 0. \end{aligned}$$

In this case, instead of minimising power losses or generation costs, as it is often the case in OPF studies, the problem consists of minimising the deviation μ_2 from the original load allocation. Although the feasible set of this problem is non-convex and, consequently, the global minimum of μ_2 might not be found, this is not critical, since a local minimum would still present sufficient similarity to the original allocation. Given that the number of buses in a LVN and thus of decision variables in the OPF problem is in the order of a few hundreds, a Sequential Quadratic Programming (SQP) method, which is appropriate for medium-range problems, is used for the solution.

Depending on the original load allocation, it is possible that the voltage constraints cannot be satisfied, especially in scenarios with high DER or load penetration and in which the power is consumed mostly at buses far from the feeder. This is solved by changing the tap position r of the MV/LV transformer that feeds each LVN, which can take any value in $\{r_{-n_1}, \ldots, r_{-1}, r_0, r_1, \ldots, r_{n_2}\}$. In order to avoid turning the OPF into a mixed-integer optimisation problem, a first attempt is made to solve it with the tap position r_i (starting with $i = 0$). If at least one voltage is lower than $\underline{v}$, then r is updated to r_{i-1} and another attempt is made; otherwise, if at least one voltage is higher than $\bar{v}$, then r is updated to r_{i+1}, and if there are both undervoltages and overvoltages, then the correction of the latter is given priority and r is updated to r_{i+1}. This priority is based on a preference of undervoltages over overvoltages, since the latter can, in reality, damage equipment. The process is repeated until either all the voltages are correct or a total of $\max(n_1, n_2)$ attempts have been made, at which point the last decision variables $\mathbf{x}'_p$ and $\mathbf{x}'_q$ are taken as a solution.

TABLE I
FINAL DER AND LOAD ALLOCATION.

	Allocated active power (kW)				
	Min.	Avg.	Max.	Total	f_d
Inverted-based AC	0.3	0.9	1.4	132.4	0.15
Conventional AC	1.0	1.4	2.0	65.5	0.15
PV system	1.9	4.5	7.3	685.6	0.15
Miscellaneous loads	3.0	4.0	5.0	2490.0	0.60
Mismatch loads	0.0	0.0	0.1	14.1	—

After the OPF has been solved, the templates in $\mathcal{M}^\star$, with their modified demands $\mathbf{x}'_p$ and $\mathbf{x}'_q$, are connected to the MV bus, thus becoming part of the bulk power system model. After applying this methodology to the MV loads in the TD system, the result would be a synthetic network with a size in the order of $1,000,000$ buses. Each bus would have a set of assigned DERs and loads, and its voltage and demand would produce a realistic simulation of the entire network. If desired, each LV load might be further disaggregated into its component DERs and loads by using the allocation functions $p(L, d)$ and $q(L, d)$. In general, in order to preserve the predefined powers in spite of the load reallocation, it is necessary to include a mismatch load $M_i = x'_{pi} - x_{pi}$ at each load bus L_i. However, this mismatch load is usually negligible in comparison with the other DERs and loads connected to the corresponding bus.

IV. TEST CASES

In this section, we present the results of disaggregating eight MV loads of the extended system presented in [7].

A. Power flow results

First, as explained in Section III-A, the base set of 14 LVN models was diversified by adding 100 additional templates. Then, as explained in Section III-B, flexible DERs and loads were allocated at each load bus: inverter-based AC units, conventional AC units, and PV systems, all of them with a penetration level $f_d = 0.15$. Inverter-based AC units were always assigned an active power in the range 0.35–$1.4\,\mathrm{kW}$ and were assumed to operate at a power factor of 0.98 lagging. Conventional AC units were assigned an active power in the range 1–$2\,\mathrm{kW}$ with a probability of 0.2, which is an approximation of their duty cycle, and were assumed to operate at a power factor of 0.95 lagging. PV systems were assigned an active power somewhere between 70% and 80% of their rated capacities, which were in turn taken from a normal distribution with $\mu = 6\,\mathrm{kW}$ and $\sigma = 1.15\,\mathrm{kW}$, and were assumed to operate at unity power factor. Finally, miscellaneous, non-flexible loads in the range 3.0–$5.0\,\mathrm{kW}$ at unity power factor were also allocated with a penetration level $f_d = 0.6$.

The resulting DER and load allocation is summarised in Table I. On average, inverter-based AC units demand less power than conventional AC units, since they operate continuously and thus require less power to maintain a given temperature. However, at the instant at which the power flow was computed,

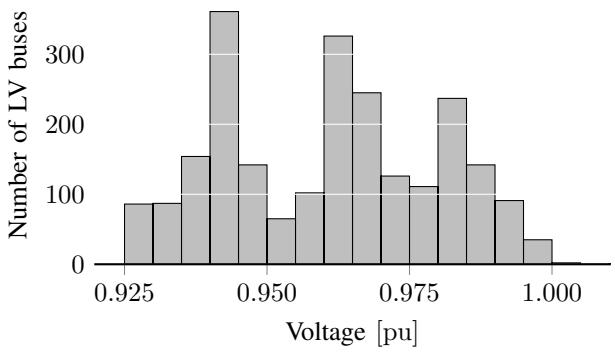

Fig. 4. Distribution of initial voltages in the LVNs. There are a total of 2313 low-voltage buses, 1050 of which are load buses.

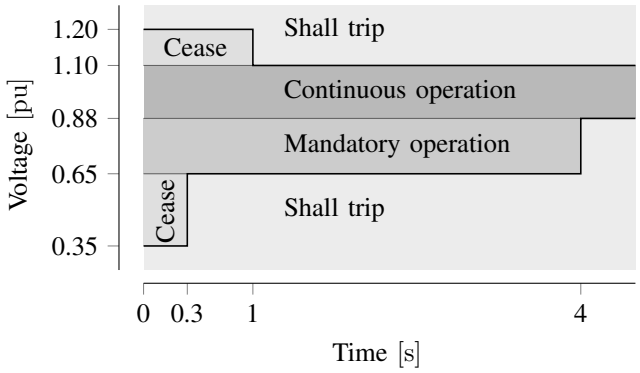

Fig. 5. LVRT and HVRT curves used by the PV systems. With the exception of the threshold for the permissive operation, which was set to 0.35 to facilitate the tripping of several units, all values are based on the IEEE-1547-2018 [19].

they demand almost twice as much power as the conventional AC units. This is due to the fact that the duty cycle of the former is 100%, while the duty cycle of the latter is approximately 20%.

The resulting LVNs were used to disaggregate eight MV loads of the TD system, located in one MV network that is fed by the transmission bus 4047. These loads were chosen to be both near and far from the HV/MV transformer in order to ensure a diverse voltage profile. After the disaggregation, a total of 14 LVNs were required and, in order for their power to match the MV load exactly, the mismatch loads shown in Table I had to be introduced. The tap positions of the MV/LV transformers had to be adjusted to keep all voltages between the bounds $\underline{v} = 0.925\,\text{pu}$ and $\bar{v} = 1.05\,\text{pu}$. This restriction was satisfied by performing one change in five of the 14 LVNs and lead to the voltage distribution shown in Fig. 4.

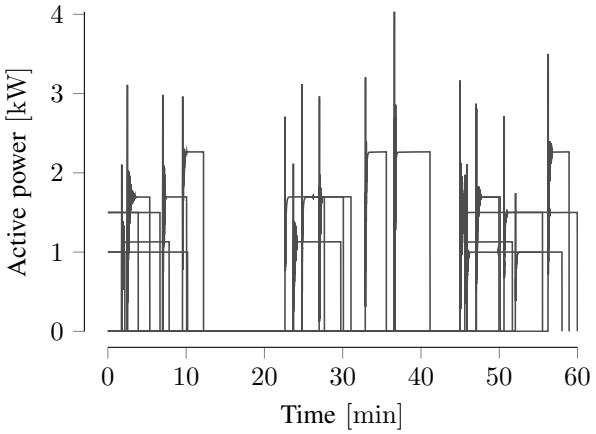

Fig. 6. Active power consumed by conventional AC units during normal operation. Out of the 152 units that were allocated throughout the LVNs, only ten units chosen at random are shown.

B. Dynamic simulations

Once the power flow results were computed, they were used as the initial condition for dynamic simulations. These simulations were carried out in RAMSES, a simulator that uses a topologically-based, domain decomposition method to partition the system and solve the subproblems defined over each subdomain, while treating the interface variables with a Schur-complement approach. In order to reduce the running time, it employs parallel computing techniques.

The DERs and loads are modeled individually by an initial-value problem for non-linear differential and algebraic equations. On the one hand, the conventional AC units are governed electrically by the dq equations of the induction machine and thermally by a two-mass model. The inverter-based AC is controlled by the PI scheme described in [15], while the conventional AC is controlled by a thermostat, as described in [16]. In order to obtain realistic and independent temperature trajectories, each thermal subsystem employs a random set of parameters that follows the guidelines given in [17] for TCLs. On the other hand, the miscellaneous loads demand a power that depends on their initial demand P_0 and Q_0 and on their initial voltage V_0 according to the exponential models

$$P = P_0 \left(\frac{V}{V_0}\right)^{\alpha} \quad \text{and} \quad Q = Q_0 \left(\frac{V}{V_0}\right)^{\beta}.$$

The exponents $\alpha = 1.5$ and $\beta = 2.5$ were used in order to model voltage dependence.

The PV systems are modeled using a variant of the DER_A, a generic model recommended by the WECC and NERC and documented in [18]. Among other features, each unit integrates its own volt-var curve, a PI controller for reactive power, and low-voltage and high-voltage ride-through (LVRT and HVRT) curves. However, unlike in the DER_A, the LVRT and HVRT curves trip the entire DER instead of tripping just a fraction, since this variant is intended to represent individual units. These features make it possible to capture the main dynamics of PV systems in response to voltage disturbances even at the LV level. All the allocated units used the same LVRT and HVRT curves, which are shown in Fig. 5. The volt-var curves were adjusted individually so that the voltages computed during the power-flow study were located inside their deadband.

The system was first simulated without any disturbance in order to test the dynamic simulation of each individual

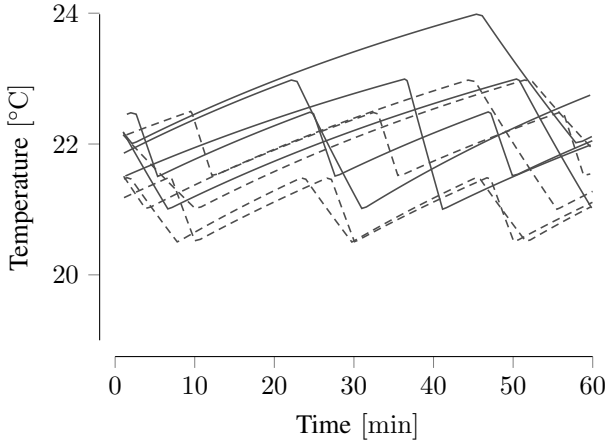

Fig. 7. Room temperatures controlled by conventional AC units. Only ten curves chosen at random are shown. The thermostats were programmed to keep the temperatures within a deadband of either 1 °C or 2 °C around a setpoint of either 21 °C, 22 °C or 23 °C. The outside temperature is 30 °C.

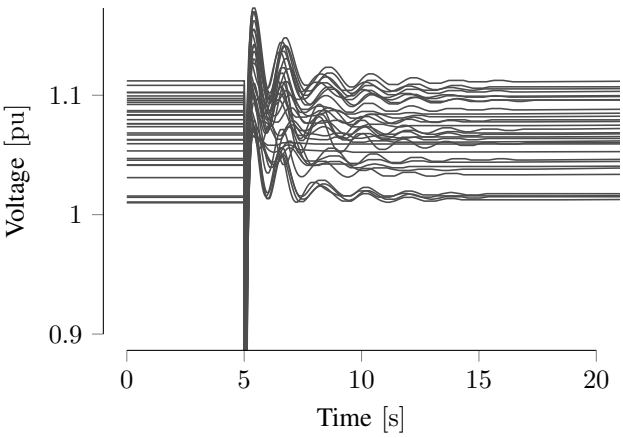

Fig. 8. TN voltages after five-cycle short circuit at the transmission bus 4044.

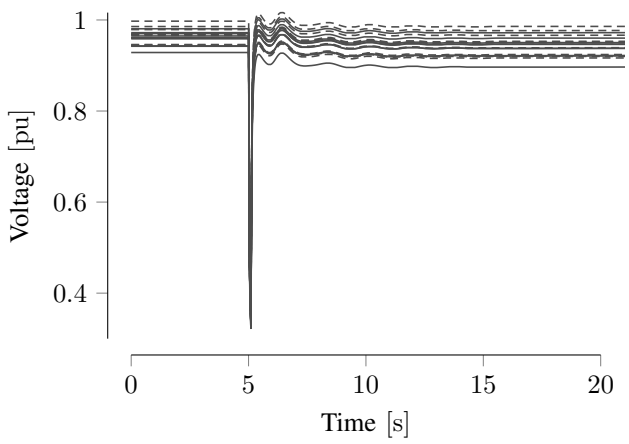

Fig. 9. Voltages measured by the PV units at their terminals during the disturbance in the TN. Out of the 152 units that were allocated throughout the LVNs, only twenty units chosen at random are shown.

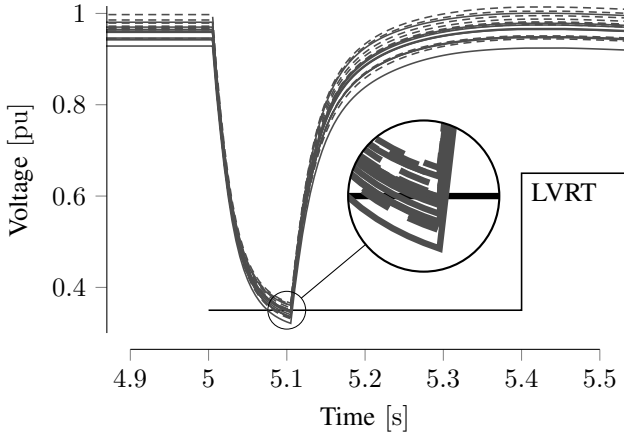

Fig. 10. Detailed view of the voltages shown in Fig. 9, which were measured by the PV units during the disturbance.

model. Figure 6 shows the active power consumption of ten conventional AC units chosen at random. Shortly after switching on, the induction motors draw an inrush current and thus present a peak in their consumption. Once they reach the steady state, their consumption settles to a value close to their rated power. As expected, these units turn on and off continuously, with a duty cycle close to 20%. Figure 7 shows the room temperatures controlled by these same units. Since each trajectory is independent, this network model is suitable for testing load control strategies that rely on the instantaneous temperature of each TCL while also taking into account the dynamics of the bulk power system.

In order to test the response of the PV systems, the TN was then subject to a large disturbance that did not produce instability. At $t = 5\,\mathrm{s}$, a five-cycle ($100\,\mathrm{ms}$) short circuit was simulated near TN bus 4044 and was cleared by opening line 4043-4044. Figure 8 shows the evolution of the TN voltages during and after the disturbance. The response is simulated over a horizon of $20\,\mathrm{s}$, which is enough to reach steady-state.

Figure 9 shows the terminal voltages of twenty PV systems. Since each system is located at a different bus of the LVNs, the voltages are evenly spread in the range 0.925–$1.00\,\mathrm{pu}$ both before and after the disturbance. Furthermore, the voltages settle at a lower value after the disturbance due to the opening of line 4043-4044. Figure 10 shows these terminal voltages in detail, along with the LVRT curve. Given that these are not real voltages but rather measurements taken by the PV units at their terminals and that the measurements were modeled by first-order delay blocks, the sudden voltage drop that follows the disturbance is perceived as an exponential decay.

The effect of the disturbance on the PV systems is shown in Fig. 11. The units first reduce their active power injection due to the drop in terminal voltage, then they cease to energize as they enter the region of permissive operation, and finally, after the fault has been cleared, some units return to inject power while others remain tripped (shown as zero injections after the tripping). They respond independently both in time and magnitude, according to their own nominal power and terminal

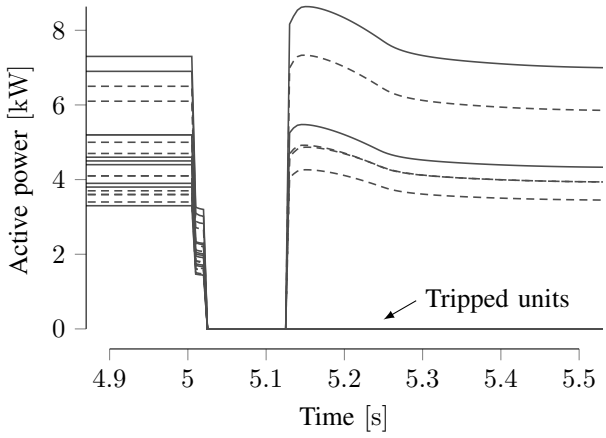

Fig. 11. Active power injection of the PV units during the disturbance. Only twenty curves chosen at random are shown.

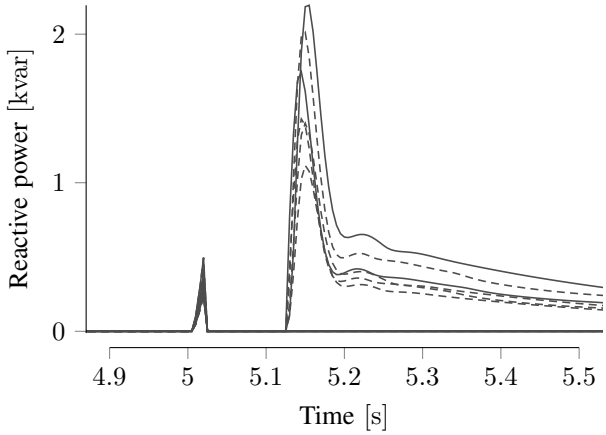

Fig. 12. Reactive power injection of the PV units during the disturbance. Only twenty curves chosen at random are shown.

conditions. A similar behaviour is observed in the reactive power response of Fig. 12. Due to the sudden voltage drop, the units inject reactive power according to their terminal voltage and their own volt-var curve in order to support the system. This injection is interrupted when the unit ceases to energize, but it is then resumed after the fault has been cleared. The reactive power settles at a non-zero value because the terminal voltages are lower after the disturbance.

V. Conclusion

This paper has presented a step forward in the creation of a network model that represents realistically and in great detail the behaviour of the entire power system. From a TD test system, eight aggregate MV loads were disaggregated into fully-modelled LVNs with flexible loads and DERs. Given the large amount of DERs that DNs will host in the future, a realistic model like the one presented in this paper is valuable for studying the ability of DERs to provide ancillary services.

The dynamic simulations considered the individual response of each flexible load and DER, subject to their own physical and local constraints. Future work will focus on applying the proposed methodology to all the MV loads presented in [7]. In such a detailed system, it will be possible to test coordination schemes for independent DERs that will be controlled and used to participate in voltage stability support.

References

[1] H. Sun, Q. Guo, J. Qi, V. Ajjarapu, R. Bravo, J. Chow, Z. Li, R. Moghe, E. Nasr-Azadani, U. Tamrakar, G. N. Taranto, R. Tonkoski, G. Valverde, Q. Wu, and G. Yang, "Review of challenges and research opportunities for voltage control in smart grids," *IEEE Transactions on Power Systems*, vol. 34, no. 4, pp. 2790–2801, 2019.

[2] T. Van Cutsem, M. Glavic, W. Rosehart, C. Canizares, M. Kanatas, L. Lima, F. Milano, L. Papangelis, R. A. Ramos, J. A. Dos Santos, B. Tamimi, G. Taranto, and C. Vournas, "Test systems for voltage stability studies: IEEE Task Force on Test Systems for Voltage Stability Analysis and Security Assessment," *IEEE Transactions on Power Systems*, pp. 1–1, 2020.

[3] B. Badrzadeh, Z. Emin, E. Hillberg, D. Jacobson, L. Kocewiak, G. Lietz, F. da Silva, and M. Val Escudero, "The need for enhanced power system modelling techniques and simulation tools," *CIGRE Science & Engineering*, vol. 17, no. Febr, pp. 30–46, 2020.

[4] J. Peppanen, C. Rocha, J. A. Taylor, and R. C. Dugan, "Secondary low-voltage circuit models—How good is good enough?" *IEEE Transactions on Industry Applications*, vol. 54, no. 1, pp. 150–159, 2017.

[5] G. Valverde, A. Argüello, R. González, and J. Quirós-Tortós, "Integration of open source tools for studying large-scale distribution networks," *IET Generation, Transmission & Distribution*, vol. 11, no. 12, pp. 3106–3114, 2017.

[6] J. Kays, A. Seack, T. Smirek, F. Westkamp, and C. Rehtanz, "The generation of distribution grid models on the basis of public available data," *IEEE Transactions on Power Systems*, vol. 32, no. 3, pp. 2346–2353, 2016.

[7] N. Pilatte, P. Aristidou, and G. Hug, "TDNetGen: An open-source, parametrizable, large-scale, transmission, and distribution test system," *IEEE Systems Journal*, vol. 13, no. 1, pp. 729–737, 2019.

[8] R. D. Zimmerman, C. E. Murillo-Sánchez, and R. J. Thomas, "MATPOWER: Steady-state operations, planning, and analysis tools for power systems research and education," *IEEE Transactions on power systems*, vol. 26, no. 1, pp. 12–19, 2010.

[9] F. Escobar. (2020) An open-source tool for disaggregating medium-voltage loads. [Online]. Available: https://github.com/franescobar/mvlodis

[10] P. Aristidou, S. Lebeau, and T. Van Cutsem, "Power system dynamic simulations using a parallel two-level schur-complement decomposition," *IEEE Transactions on Power Systems*, vol. 31, no. 5, pp. 3984–3995, 2015.

[11] Distributed Generation and Sustainable Electrical Energy Centre. (2015) United Kingdom Generic Distribution System (UK GDS). [Online]. Available: https://github.com/sedg/ukgds

[12] C. Fennan, "Creation of a generic test case for combined simulations of medium and low voltage networks," ETH Zürich, Semester thesis, 2018.

[13] M. Pipattanasomporn, M. Kuzlu, S. Rahman, and Y. Teklu, "Load profiles of selected major household appliances and their demand response opportunities," *IEEE Transactions on Smart Grid*, vol. 5, no. 2, pp. 742–750, 2013.

[14] R. Bellman, "Notes on the theory of dynamic programming IV-Maximization over discrete sets," *Naval Research Logistics Quarterly*, vol. 3, no. 1-2, pp. 67–70, 1956.

[15] H. Hui, Y. Ding, and M. Zheng, "Equivalent modeling of inverter air conditioners for providing frequency regulation service," *IEEE Transactions on Industrial Electronics*, vol. 66, no. 2, pp. 1413–1423, 2018.

[16] D. Weber, "Modeling and simulation of flexible loads for control of distribution networks," ETH Zürich, Semester thesis, 2018.

[17] D. P. Chassin, J. C. Fuller, and N. Djilali, "GridLAB-D: An agent-based simulation framework for smart grids," *Journal of Applied Mathematics*, vol. 2014, 2014.

[18] "Reliability guideline: Parametrization of the DER_A model," North American Electric Reliability Corporation, Atlanta, Tech. Rep., 2019.

[19] "IEEE standard for interconnection and interoperability of distributed energy resources with associated electric power systems interfaces," *IEEE Std 1547-2018 (Revision of IEEE Std 1547-2003)*, pp. 1–138, 2018.